Sensors and Actuators B 190 (2014) 865–872

Contents lists available at ScienceDirect

Sensors and Actuators B: Chemical

journal homepage: www.elsevier.com/locate/snb

Flexible NO_2 sensors fabricated by layer-by-layer covalent anchoring and in situ reduction of graphene oxide

Pi-Guey Su*, Hung-Chiang Shieh

Department of Chemistry, Chinese Culture University, Taipei 111, Taiwan

ARTICLE INFO

Article history:
Received 13 May 2013
Received in revised form
14 September 2013
Accepted 17 September 2013
Available online 25 September 2013

Keywords:
Flexible NO_2 sensor
Layer-by-layer (LBL)
In situ reduction
Graphene oxide (GO)
Covalently bonding

ABSTRACT

Novel flexible NO_2 gas sensors were fabricated by covalently bonding graphene oxide (GO) to a gold electrode on a plastic substrate using a peptide chemical protocol and then reducing in situ GO film to a reduced GO (RGO) film. A pair of comb-like Au electrodes on a polyethylene terephthalate (PET) substrate were pretreated with cysteamine hydrochloride (CH) and then reacted with GO using N-(3-dimethylaminopropyl)-N′-ethylcarbodiimide hydrochloride (EDC) and *N*-hydroxysuccinimide (NHS) as the peptide coupling reagent, before undergoing a final reduction by sodium borohydride ($NaBH_4$). The anchored RGO film was characterized by atomic force microscopy (AFM), scanning electron microscopy (SEM), electrochemical impedance spectroscopy (EIS) and Fourier transform infrared spectroscopy (FTIR). The gas sensing properties, including sensitivity, sensing linearity, reproducibility, response time, recovery time, cross-sensitivity effects and long-term stability, were investigated. Interfering gas NH_3 affected the limit of detection (LOD) of a target NO_2 gas in a real-world binary gas mixture. The flexible NO_2 gas sensor exhibited a strong response and good flexibility that exceeded that of sensors that were made from graphene film grown by chemical vapor deposition method (CVD-graphene) at room temperature. Its use is practical because it is so easy to fabricate.

1. Introduction

Graphene is composed of a two-dimensional (2D) array of carbon atoms that are covalently connected via sp2 bonds to form a honeycomb sheet [1]. Graphene has been widely used in batteries, supercapacitors, nanoelectronic and electrochemical sensors because of its high mechanical strength, high surface area, high electron mobility at room temperature and low manufacturing cost [1–3]. Graphene oxide (GO) sheets have recently become attractive as possible intermediates in the manufacture of grapheme [4]. GO surface functionalization is important in controlling the exfoliation behavior of graphene oxide and reduced graphene oxide (RGO). Therefore, GO has various applications, including gas sensors [5], and many groups have used graphene-based sensing materials to detect various chemical species, such as NO_2, NH_3, H_2 and CO_2 [6–12]. In many related works, graphene-based coatings were deposited on rigid substrates, such as glass, ceramics or silicon wafer. The rigidity of these sensors based on rigid substrates makes them unsuitable for application in various new areas, such as handheld portable consumer electronics, aeronautic transportation and civil engineering, that require flexible, lightweight and mechanical shock-resistive sensing elements [13,14]. Additionally, flexible multisensor platforms that support temperature, humidity and gas detection can be manufactured at very low cost and integrated into smart textiles or radio frequency identification (RFID) tags [15,16]. The development of sensors in the future should be consistent with the goal of complete flexibility, and extensibility to the sensing of various gases. The main challenges not only concern their manufacture, but also the stability of their mechanical, electrical and gas-sensing properties of these devices under repeated bending. The sensing characteristics of a flexible gas sensor depend on its microstructure, which is determined by its fabrication process. Recently, Kim et al. fabricated a flexible NO_2 gas sensor by spin-coating chemical vapor-deposited graphene (CVD-graphene) with poly(methyl methacrylate) (PMMA) on a polyethylene terephthalate (PET) substrate [17]. Kang et al. fabricated a flexible H_2 gas sensor by spin-coating CVD-graphene that was decorated with palladium (Pd) nanoparticles on a PET substrate [18]. These fabrication techniques are complex and costly.

Layer-by-layer self-assembly (LBL-SA) method is based on sequential electrostatically adsorptions of ionized polyelectrolytes and oppositely charged materials in aqueous solutions. LBL self-assembly has many advantages over other methods, including simplicity, low-cost, low temperature of deposition, controllable thickness (from nanometers to micrometers) and the need for no complex equipment [19–21]. This approach has recently been adopted to fabricate multi-walled carbon nanotubes (MWCNTs)-glucose oxidase multilayers and SWCNTs on flexible substrates as

* Corresponding author. Tel.: +886 2 28610511x25332; fax: +886 2 28614212.
E-mail addresses: spg@faculty.pccu.edu.tw, spg@ulive.pccu.edu.tw (P.-G. Su).

0925-4005/$ – see front matter © 2013 Elsevier B.V. All rights reserved.
http://dx.doi.org/10.1016/j.snb.2013.09.078

flexible glucose biosensors [22] and piezoresistive type sensors [23], respectively. In our earlier works [24–27], flexible NO_2, NH_3 and H_2 sensors were fabricated by the LBL assembly of MWCNTs or polypyrrole (PPy) on PET substrates. However, the performance of flexible gas sensors is worsened by long-term use because the sensing films are not anchored to the substrate. In recent years, since new peptide coupling reagents have been developed for use in organic synthesis, peptide coupling reactions have been widely studied. In a typical peptide coupling reaction, a carboxyl group of a compound is initially activated by a suitable peptide coupling reagent, and it is subsequently reacted with an amine group in another compound [28]. Kwak et al. fabricated a hydrogen peroxide sensor that was made by bonding polyamidoamine (PAMAM) dendrimer onto thiol-modified gold electrodes on a Si wafer using N-(3-dimethylaminopropyl)-N′-ethylcarbodiimide hydrochloride (EDC) as a peptide coupling reagent [29]. In our earlier work [30], a flexible humidity sensor was fabricated by the LBL anchoring of a copolymer of methyl methacrylate (MMA) and [3-(methacrylamino)propyl] trimethyl ammonium chloride (MAPTAC) film on a 3-mercaptopropionic acid (MPA)-modified Au electrode (MPA/Au) on a PET substrate. However, no attempt has been made to anchor the GO onto a gold electrode on a flexible substrate and then to perform the in situ reduction of GO to fabricate flexible NO_2 sensors. In this work, a GO film was covalently anchored onto the cysteamine hydrochloride (CH)-modified gold electrode on a PET substrate using EDC and *N*-hydroxysuccinimide (NHS) (EDC/NHS) as the peptide coupling reagent, and this film was reduced in situ by sodium borohydride ($NaBH_4$) to form an RGO film yielding a flexible NO_2 gas sensor. The films were characterized by atomic force microscopy (AFM), scanning electron microscopy (SEM), Fourier transform infrared spectroscopy (FTIR) and the electrochemical impedance spectroscopy (EIS). The effect of the duration of reduction of GO film on the electrical properties of the film was investigated. The flexibility and gas sensing properties, such as sensitivity, sensing linearity, reproducibility, response time, recovery time, cross-sensitivity effects and stability of the sensor were investigated.

2. Experimental

2.1. Materials

Graphene oxide (GO; 5 g/L, UniRegion Bio-Tech) were used without further purification. Cysteamine hydrochloride (95%; CH), N-(3-dimethylaminopropyl)-N′-ethylcarbodiimide hydrochloride (95%; EDC), *N*-hydroxysuccinimide (95%; NHS) and sodium borohydride (95%; $NaBH_4$) were obtained from Aldrich. All reagents used were analytical grade. All used deionized water (DIW) was prepared using a Milli-Q Millipore (Bedford, MA, USA) purification system, and the resistivity of water was above 18.0 MΩ cm^{-1}.

2.2. Fabrication of flexible NO_2 sensor

Fig. 1(a) displays a picture of the structure of NO_2 sensors fabricated on a PET substrate. The interdigitated gold electrodes were made by sputtering initially Cr (thickness 50 nm) and then Au (thickness 250 nm) in a temperature range of 120–160 °C. The electrode gap was 0.2 mm. The substrates were firstly treated with an H_2O_2/H_2SO_4 mixture (1:2, 15 mL), washed in de-ionized water (DIW) and then cleaned in acetone solution for 3 min. The pretreated substrate was immersed in 2.0 mM ethanol solution of CH (75/25% ethanol/DIW) for 24 h at room temperature and then washed thoroughly in 75/25% ethanol/DIW to remove the non-chemisorbed materials. It was then dried at 80 °C to yield a CH-modified electrode (CH/Au). Then, the CH/Au was immersed

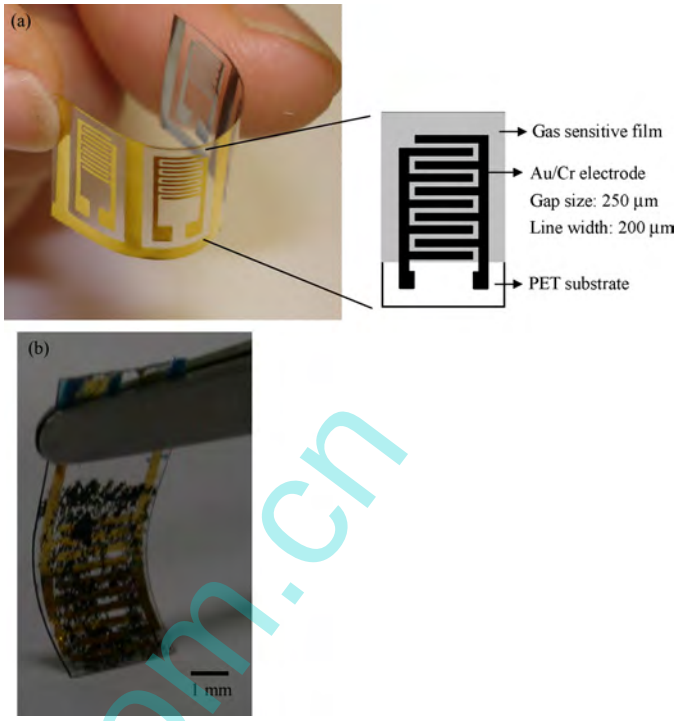

Fig. 1. (a) Structure of flexible gas sensor; (b) Photograph of bent gas sensor based on RGO film anchored on a PET substrate.

in 50 μL of GO solution (5 g/L) that contained 200 mM EDC and 400 mM NHS for 12 h at room temperature. It was then washed thoroughly in DIW to remove any non-anchored GO to form GO-CH/Au. The as-prepared anchored GO film was reduced by immersing the GO-CH/Au substrate in aqueous $NaBH_4$ (0.04%) for 5 min, rinsing it with DIW and then drying it at 80 °C. Fig. 1(b) shows the flexibility of the RGO film that was covalently anchored and reduced in situ on a PET substrate. Fig. 2 schematically depicts the fabrication of a flexible NO_2 sensor by the LBL covalent anchoring and the in situ reduction of GO on a PET substrate.

2.3. Instruments and analysis

An infrared spectrometer (Nicolet 380) was used to obtain the IR spectra of the covalently anchored GO and RGO films. A standard three-electrode cell, connected to an electrochemical workstation (ZAHNER ZENNIUM, Germany), was used to make the electrochemical measurements. All electrochemical measurements were made in the presence of a 10 mM $K_3[Fe(CN)_6]/K_4[Fe(CN)_6]$ (1:1) mixture (with 0.2 M NaCl as the supporting electrolyte). The applied voltage as 0.2 V and frequency range from 10 mHz to 10 kHz at 25 °C were chosen for the electrochemical impedance spectra analysis. The surface microstructure of the thin film that was coated on a PET substrate was investigated using a field emission scanning electron microscope (FEI company, Nova NanoSEM^{TM} 230) and an atomic force microscope (AFM, Ben-Yuan, CSPM 4000) in tapping mode which the horizontal and vertical resolution are 0.26 and 0.10 nm, respectively. The electrical and sensing characteristics were measured using a bench system at room temperature, as shown in Fig. 3. Each sensor was connected in series with a load resistor and a fixed 5 V tension (DC mode) was continuously supplied to the sensor circuit from a power supply (GW, PST-3202). The resistance of the sensor was determined from the voltage at the ends of the load resistor using a DAQ device (NI, USB-6218) in various concentrations of gas. The standard NH_3, CO, H_2 and NO_2 gases which we used here for investigation were purchased from Shen Yi

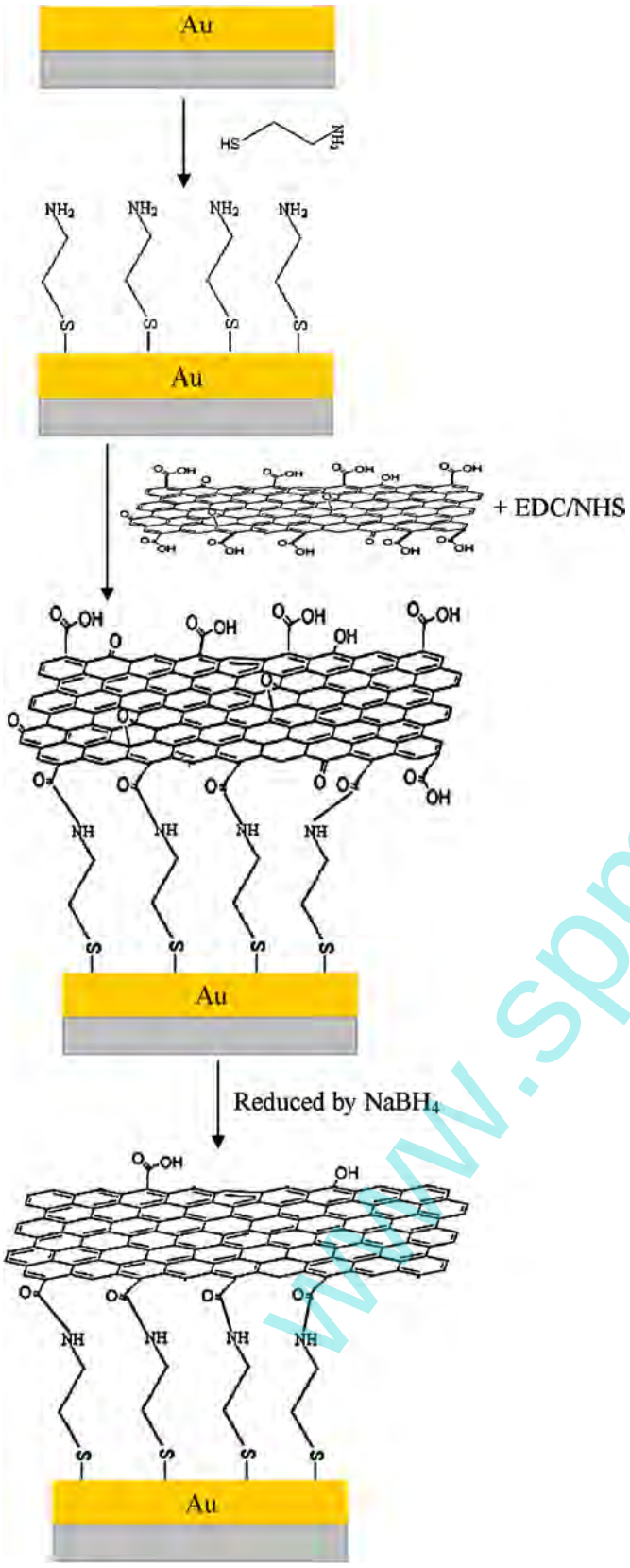

Fig. 2. Fabrication of a flexible NO_2 sensor by LBL covalent anchoring and in situ reduction of GO film to reduced GO film.

Gas Co. (Taiwan). The concentration for standard NH_3, CO, H_2 and NO_2 gases were 100,000, 100,000, 100,000 and 1000 ppm, respectively. The required various gas concentrations were produced by diluting the known volume of standard gas with dry air and then were injected into the chamber. The desired various gas concentrations were measured using a calibrated gas sensor system (Dräger, MiniWarn). The cross-sensitivity experiment was performed by measuring the resistance of the sensor exposure to NH_3, CO, H_2 and H_2O gases, respectively. The volume of the chamber is 18 L. The gas inside the chamber was uniformly distributed using a fan. After some time, the chamber was purged with air and the experiment was repeated for another cycles. All experiments were performed at room temperature, which was about $23.0 \pm 1.5\,^{\circ}C$ and the relative humidity was $53 \pm 3\%$ RH. Flexibility experiments were performed in which the sensors were bent to various degrees as their responses were monitored as a function of the period of exposure to NO_2 gas. The bending angle was measured using a goniometer. The sensor response (S) was calculated by the following equation:

$$S(\%) = \frac{R_{gas} - R_{air}}{R_{air}} \times 100\% = \frac{\Delta R}{R_{air}} \times 100\% \quad (1)$$

where R_{gas} and R_{air} are the electrical resistances of the sensor in the tested gas and air, respectively.

3. Results and discussion

3.1. Preparation and characterization of LBL covalent anchoring and in situ reduction of GO film

Fig. 2 shows the layer-by-layer procedure for covalent anchoring GO onto the thiol-modified gold electrode and then reducing it in situ using conventional peptide chemical protocols. Firstly, the CH monolayer was chemisorbed onto the gold electrode surface, forming a gold–thiolate bond. Then, GO was covalently anchored to the surface of the CH-modified gold electrode by forming a peptide bond: the carboxylic acid groups in the GO were activated by EDC/NHS (peptide coupling reagent), which reacted with amine groups in the CH-modified gold electrode to form chemical amide bonds. Finally, the covalently GO-CH-modified electrode was further reduced in situ by $NaBH_4$ to yield reduced GO-CH/Au electrode (RGO-CH/Au).

3.1.1. Microstructure of surface

The surface morphology of the LBL covalently anchored RGO film was investigated by AFM. Fig. 4 shows the AFM of the LBL covalently anchored RGO film on a PET substrate. The root mean square (RMS) roughness of the LBL anchored RGO film was 10.5 nm. AFM analysis

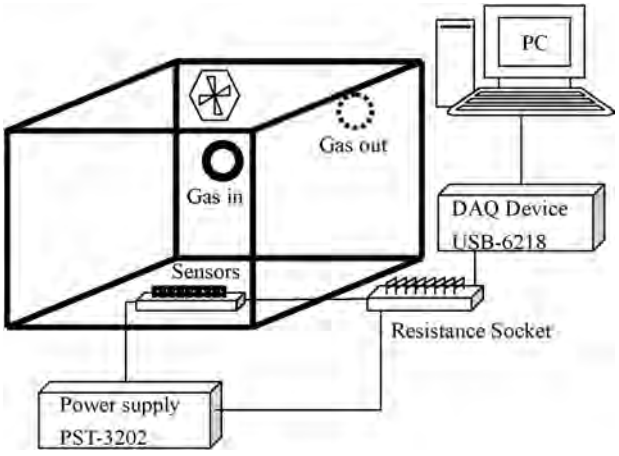

Fig. 3. Measurement system for testing gas sensors.

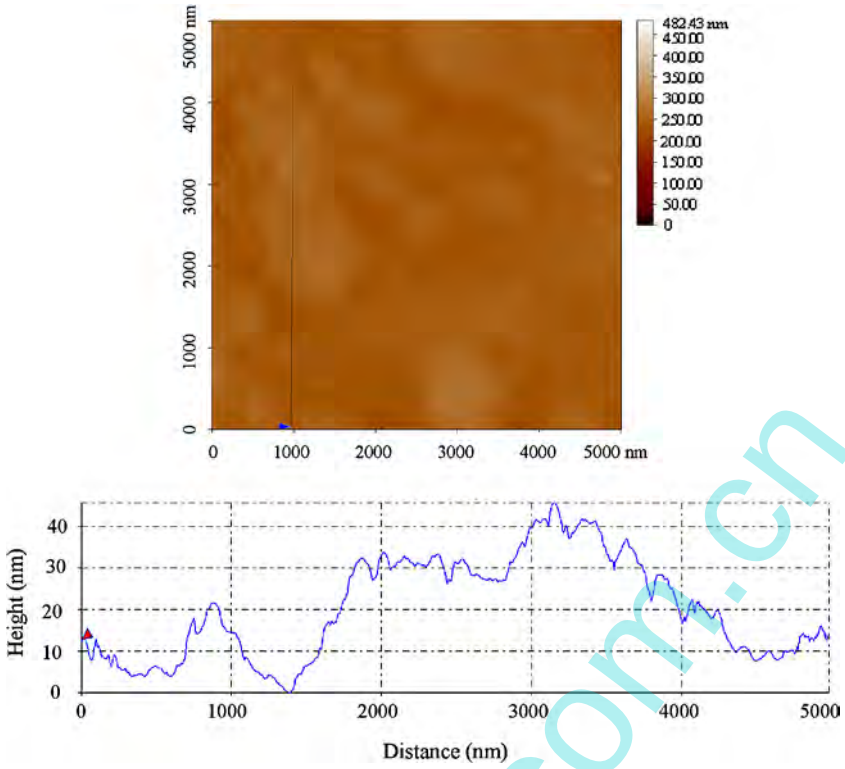

Fig. 4. AFM image of LBL covalently anchored RGO film.

revealed that its thickness was 10–30 nm. Fig. 5 shows the SEM image of the film on a PET substrate. Clearly, multi-layered RGO with a flakelike and wrinkled structure was covalently anchored onto the substrate.

3.1.2. Electrochemical analysis

Electrochemical impedance spectra (EIS) were obtained to characterize the interface properties of the modified electrodes. In EIS, the diameter of the semicircle at higher frequencies in the Nyquist diagram that was obtained by impedance spectroscopy yields the interfacial electron transfer resistance (Ret), which determines the electron transfer kinetics of the redox probe at the electrode surface. Fig. 6 plots the Nyquist diagrams of EIS of the bare Au electrode, the CH/Au electrode and the RGO-CH/Au electrode. The bare Au electrode exhibited a high Ret of about 37 kΩ because the electrode comprised a pair of comb-like Au electrodes. As CH was chemisorbed on the Au surface, the Ret decreased to a small value about 142 Ω (inset in Fig. 6), owing to the formation of a conductive path by the interconnected MPA with itself and the positively charged amine groups of CH, which effectively attracted negatively charged $[Fe(CN)_6]^{3-/4-}$, improving the electron transfer rate. When GO was further anchored onto the surface of the CH/Au electrode and reduced in situ by $NaBH_4$, the curve was an almost straight line (inset in Fig. 6), revealing a very low resistance to interfacial electron transfer because of the formation of a new conductive path by the RGO. This phenomenon clearly suggests that the RGO film was successfully and covalently anchored onto the CH/Au surface.

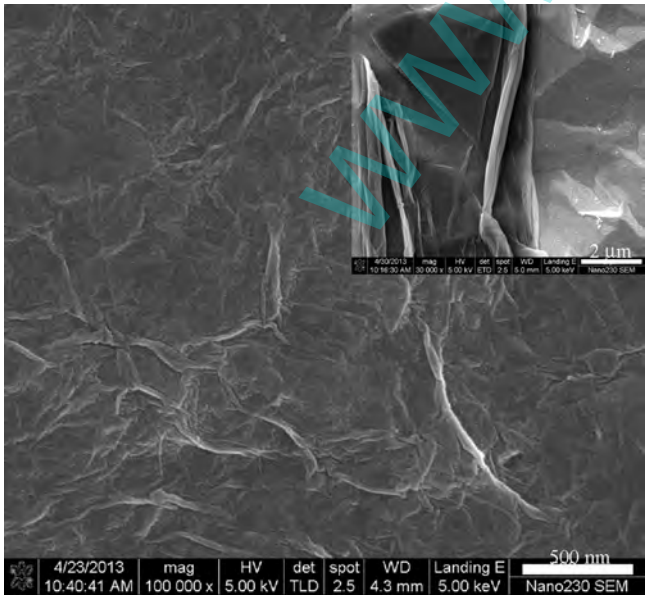

Fig. 5. FE-SEM image of LBL covalently anchored RGO film.

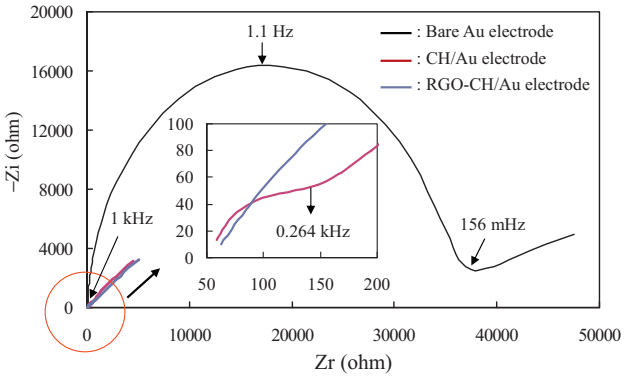

Fig. 6. Electrochemical impedance spectra of bare interdigitated electrode, CH/Au electrode, and RGO-CH/Au electrode.

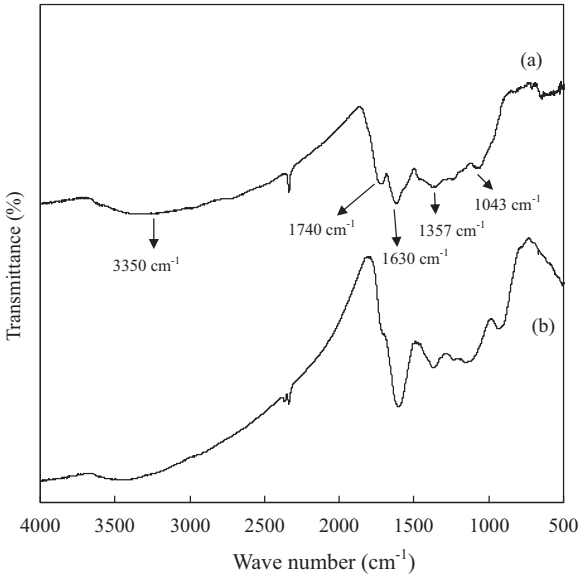

Fig. 7. IR spectra of (a) GO and (b) RGO covalently anchored onto CH/Au surface.

3.1.3. IR spectra

The GO and RGO films that were covalently anchored onto the CH/Au surface were investigated by IR spectroscopy. In Fig. 7(a), the IR spectrum of the GO that was covalently anchored onto the CH/Au surface included a peak at 3350 cm^{-1} attributable to the O—H stretching vibration, peaks at 1740 and 1630 cm^{-1} attributable to the C=O stretching vibrations, and a peak at 1357 cm^{-1} attributable to the deformation of O—H. Additionally, a peak at 1043 cm^{-1} was associated with amide (C—N) stretching in the GO that was covalently anchored onto the CH/Au surface. The band at 1740 cm^{-1} was absent from spectrum of the RGO that was covalently anchored onto the CH/Au surface (Fig. 7(b)). These results confirm that the GO was successfully covalently anchored onto the CH/Au surface and it was reduced to RGO by $NaBH_4$.

3.2. Electrical properties of LBL covalently anchored and in situ reduced of GO film

Fig. 8 plots the effect of the reduction time on resistance of the LBL covalently anchored GO film. The as-prepared LBL covalently anchored GO film exhibited a high resistance of about GΩ owing to the oxygen functional groups in its basal plane and edges. The resistance of the LBL covalently anchored GO film decreased gradually

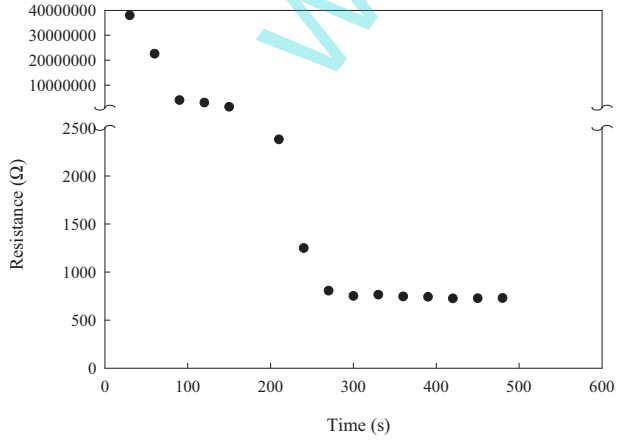

Fig. 8. Effect of reduction time on resistance of LBL covalently anchored GO film.

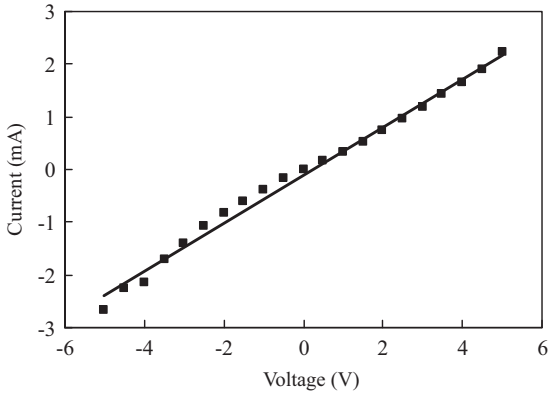

Fig. 9. I–V characteristics of LBL covalently anchored RGO film.

with its the reduction time up to 300 s, after which the resistance barely changed because all of the oxygen-containing functional groups have been eliminated [31]. Fig. 9 plots the I-V characteristics of the LBL covalently anchored RGO film. The I–V relationship was linear between −5 and 5 V, revealing good ohmic contact and tunable conductivity.

3.3. Flexibility and gas sensing properties of sensor made of LBL covalently anchored RGO film

3.3.1. Flexibility properties

Fig. 10 plots the flexibility characteristics of the sensor that was made of an LBL covalently anchored RGO film. The flexibility of the sensor was evaluated by the bending angle (θ) (inset in Fig. 10). At each indicated bending angle, the sensor was exposed to 5 ppm NO_2 gas. The response (S) of the sensor decreased when it was bent. The response (S) of the sensor when it was bent downward at an angle of up to 30° deviated by less than 4% from that measured when it was flat. However, deviation of the response (S) of the sensor increased gradually to 48% as the bending angle increased up to 50° perhaps because the covalent bonding between RGO and CH reduced the flexibility of the anchored RGO film.

3.3.2. Gas sensing properties

Fig. 11 plots the real-time response (S) curves of the flexible NO_2 gas sensor to various concentrations of NO_2. The response was reversible. Fig. 12 plots the response (S) of the flexible NO_2 gas sensor as a function of concentration of NO_2 gas. The response (S) of the flexible NO_2 gas sensor was determined after 20 min exposure to a given concentration of NO_2 gas. This curve was quite linear ($Y = 13.86\,X + 0.9921$; $R^2 = 0.9970$, where Y is the response; X is the logarithm of the concentration, and R^2 is the correlation coefficient)

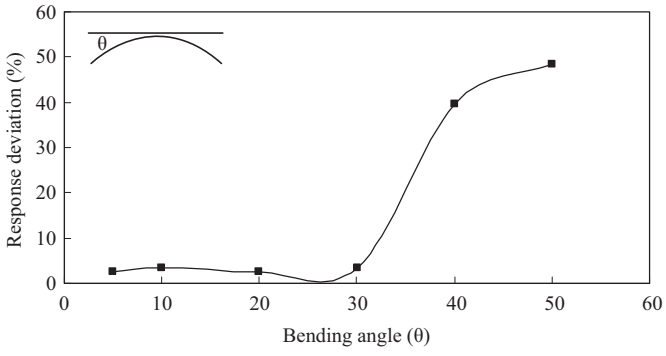

Fig. 10. Flexibility of LBL covalently anchored RGO film on PET substrate in response to 5 ppm NO_2 gas.

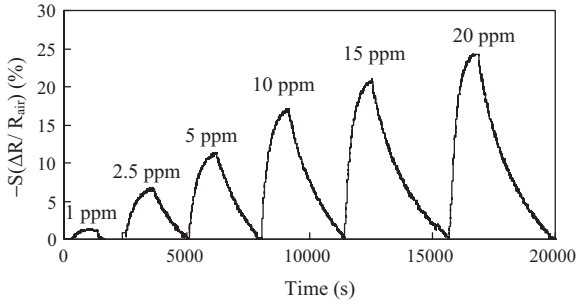

Fig. 11. Response of flexible NO_2 sensor as function of time (s) in various concentrations of NO_2 gas.

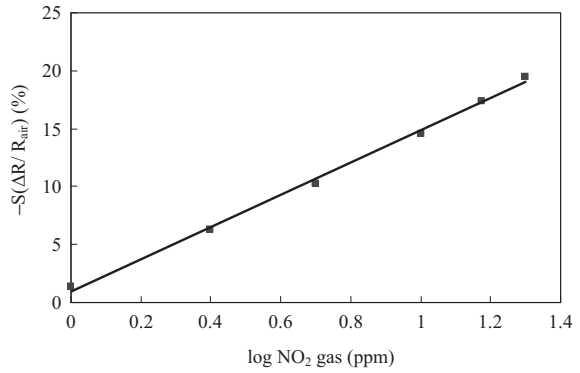

Fig. 12. Linear dependence of response of flexible NO_2 sensor on concentration of NO_2.

in the range from 1 to 20 ppm. Fig. 13 plots the real-time response of the flexible NO_2 gas sensor. The response time is defined as the time required for the sensor to reach 90% of the maximum change in resistance following exposure to a given gas. The recovery time is defined as the time required for the sensor to recover 90% of the decrease in resistance after it is exposed to a dry gas. The response and recovery times of the flexible NO_2 gas sensor herein were 7 and 28 min, respectively, at an NO_2 testing concentration of 5 ppm. Additionally, two gas on/off cycles produced similar responses, indicating the reproducibility of the flexible NO_2 gas sensor. Fig. 14 plots the results concerning the cross-sensitivity effects of NH_3, CO, H_2 and H_2O gases on the sensor. The sign of response (S) positive or negative for the considered adsorbates can be understood as indicating one of two charge transfer mechanisms. In this work, NO_2 and H_2O doped the LBL covalently anchored RGO film with holes, while NH_3, CO and H_2 doped it with electrons. Therefore, the prepared LBL covalently anchored RGO film herein exhibited the electrical behavior of a p-type semiconductor. During the sensing process, the adsorption of electron-withdrawing NO_2

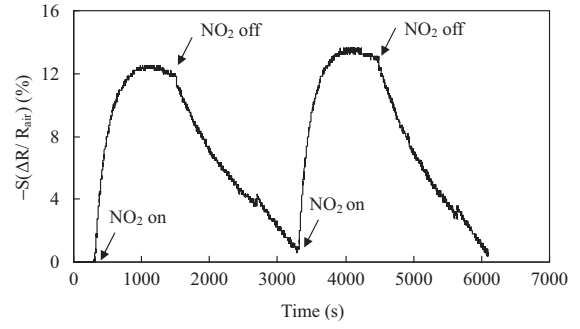

Fig. 13. Reproducibility of response of flexible NO_2 sensor to 5 ppm NO_2 gas.

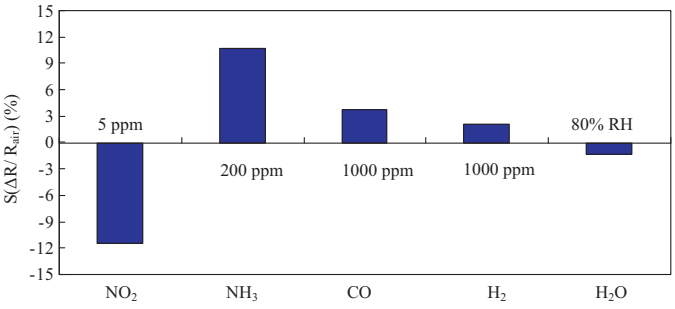

Fig. 14. Response (S) of flexible NO_2 sensor to various gases.

molecules compensates for the hole carriers in p-type RGO, causing the electrical resistance of the LBL covalently anchored RGO film to decrease with concentration of NO_2 [32–34]. This conclusion is consistent with both theoretical calculations and experimental observations that have been made by other groups [18,32–34]. The electrical resistance of the LBL covalently anchored RGO film decreased when the film was exposed to water vapor (humidity). The issue can be analyzed by considering two main effects. First, as the relative humidity (RH) is low, leading to the little water vapor adsorbed on RGO film and formed a dipole layer with the negative charges toward the RGO. The role of water vapor looks like as an oxidant (electron–acceptor), too much exposure with water vapor will cause the increase of hole density for RGO film, resulting in a significant decrease of electrical resistance in LBL covalently anchored RGO film [32–37]. Second, by further increasing the RH, the multilayered physisorbed water molecules will be formed on the surface of LBL covalently anchored RGO film, resulted in the formation of proton (H^+) and hydroxyl ions (OH^-) by dissociation process. Therefore, it was believed that the conductivity increase (resistance decrease) of the LBL covalently anchored RGO film was due to ionic contribution at high RH [38,39]. Generally, the sensing principle of the LBL covalently anchored RGO film was based on the electronic and ionic conductivity in the low and high RH, respectively. The response (S) to the CO, H_2 and H_2O gases was in each case small such that these gases may be regarded as having undetectable cross-sensitivity effects with NO_2. However, the sensor exhibited a strong response (S) (10.7) to 200 ppm of NH_3 gas so that the NH_3 gas was used herein as the interfering gas. Fig. 15 plots the response curve of the flexible NO_2 gas sensor upon exposure to a binary gas mixture of an increasing concentration of NO_2 gas and 200 ppm of the interfering gas NH_3. The electrical resistance of the sensor was reduced by exposure to NO_2 gas, but it increased upon exposure to NH_3 gas. Exposure to the selected binary gas mixture (5 ppm NO_2 plus 200 ppm NH_3) reduced the electrical resistance, such that the interaction of the NO_2 gas with the LBL covalently anchored RGO film dominated under these conditions. Therefore, at an NH_3 gas concentration of below 200 ppm, NH_3 gas may be regarded as

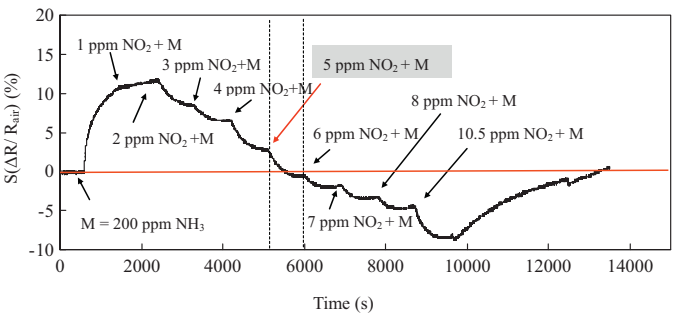

Fig. 15. Response of flexible NO_2 sensor to binary gas mixture of fixed concentration, 200 ppm of NH_3 and various concentrations of NO_2 gas from 1 to 10.5 ppm.

Table 1
Flexible NO_2 sensor performance of this work compared with the literatures.

Sensor substrate	Sensor type	Fabrication method	Sensing material	Response[d] (%)	Flexibility	References
PET	Flexible	LBL-anchored[a]	RGO	11.5[e]	4%[g]	This work
PET	Flexible	LBL-SA[b]	MWCNTs	10.3[e]	2%[h]	[24]
PET	Flexible	CVD[c]	Graphene	22.7[f]	7.7%[i]	[17]

[a] Layer-by-layer combined with a peptide chemical protocol.
[b] Layer-by-layer self-assembly.
[c] Chemical vapor deposition.
[d] The response was defined as the absolute value of response (S) under flat condition.
[e] The sensor in response to 5 ppm NO_2 gas.
[f] The sensor in response to 200 ppm NO_2 gas.
[g] The flexibility was defined as the deviation of the response (S) of the sensor was bent downward at an angle of up to 30° in relation to the measurement made when it is flat in a testing concentration of 5 ppm of NO_2.
[h] The flexibility was defined as the deviation of the response (S)of the sensor was bent downward at an angle of up to 60° in relation to the measurement made when it is flat in a testing concentration of 5 ppm of NO_2.
[i] The flexibility was defined as the deviation of the resistance of the sensor was at a strain (S) of 1.39% in a testing concentration of 200 ppm of NO_2. The strain (s) was calculated by the equation: $S = d/2r \times 100$ (%), where d is the thickness of the film and r is the radius of curvature.

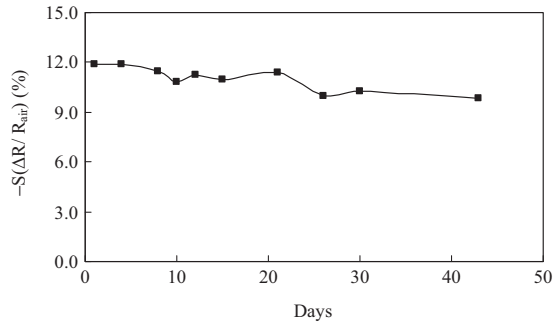

Fig. 16. Long-term stability of flexible NO_2 sensor exposed to 5 ppm NO_2 gas.

having undesirable cross-sensitivity effects with NO_2 gas at concentrations above 5 ppm. Moreover, these results reveal how the interfering gas NH_3 affects the limit of detection (LOD) of a target NO_2 gas in a real-world binary gas mixture, especially when the concentration of NO_2 gas is low. The NO_2 detection limit in a binary mixture with 200 ppm NH_3 was 5 ppm. Fig. 16 plots the long-term stability of the flexible NO_2 gas sensor. This sensor retained 86% of its original response even after 43 days in a testing concentration of 5 ppm of NO_2. Table 1 compares the NO_2 gas sensing properties of the presented flexible NO_2 sensor with those of sensors in our previous work [24] and elsewhere in the literature [17]. The response (S) and flexibility of the flexible NO_2 sensor that made of an LBL covalently anchored RGO film were greater than those of the sensor that was made of the graphene film grown by chemical vapor deposition method (CVD-graphene). However, the flexibility of the flexible NO_2 sensor that was made of the LBL covalently anchored RGO film was slightly less than that of the sensor that was made of the MWCNTs film by LBL-SA because two-cycle poly(4-styrenesulfonic acid-*co*-maleic acid)/poly(allylamine hydrochloride) (PSSMA/PAH) bilayers (precursor layer) were deposited on the substrate in the latter sensor, improving its flexibility.

4. Conclusions

FTIR and EIS analyses revealed that a novel flexible NO_2 gas sensor was successfully fabricated by the layer-by-layer covalent anchoring of a GO film and its reduction in situ to an RGO film on a modified PET substrate. Microstructural observations revealed that a multi-layered flakelike RGO film was covalently anchored onto the PET substrate. The novel flexible NO_2 gas sensor exhibited satisfactory flexibility (with only a 4% deviation in response (S) when the sensor was bent downward at an angle of up to 30°), a strong sensitivity and acceptable linearity ($Y = 13.86\,X + 0.9921$; $R^2 = 0.9970$) between 1 and 20 ppm, high reproducibility and long-term stability (for at least 43 days). The response and recovery times of the sensor were long. CO, H_2 and H_2O gases may be regarded as having unobvious cross-sensitivity effects with NO_2. However, the NH_3 gas observably influenced the response (S) of the NO_2 gas sensor especially to low concentrations of NO_2 gas (< 5 ppm). The NO_2 detection limit in a binary gas mixture with 200 ppm NH_3 was 5 ppm. The novel flexible gas sensor exhibited satisfactory sensing properties in the detection of NO_2 gas and can be practically used because of the ease and low cost of its fabrication.

Acknowledgement

The authors thank the National Science Council (grant no. NSC 100-2113-M-034-001-MY3) of Taiwan for support.

References

[1] K.S. Novoselov, A.K. Geim, S.V. Morozov, D. Jiang, Y. Zhang, S.V. Dubonos, I.V. Grigorieva, A.A. Firsov, Electric field effect in atomically thin carbon films, Science 306 (2004) 666–669.
[2] R.F. Service, Carbon sheets an atom thick give rise to graphene dreams, Science 324 (2009) 875–877.
[3] Y.Y. Shao, J. Wang, H. Wu, J. Liu, I.A. Aksay, Y.H. Lin, Graphene based electrochemical sensors and biosensors: a review, Electroanalysis 22 (2010) 1027.
[4] C. Daniela, V.D. Marcano, J.M. Kosynkin, J.M. Berlin, A. Sinitskii, Z. Sun, A. Slesarev, L.B. Alemany, W. Lu, M.J.M. Tour, Improved synthesis of graphene oxide, Nano 4 (2010) 4806–4814.
[5] S. Basua, P. Bhattacharyya, Recent developments on graphene and graphene oxide based solid state gas sensors, Sens. Actuators B 173 (2012) 1–21.
[6] M.W.K. Nomani, R. Shishira, M. Qazia, D. Diwana, V.B. Shieldsb, M.G. Spencerb, G.S. Tompac, N.M. Sbrockeyc, G. Koley, Highly sensitive and selective detection of NO_2 using epitaxial graphene on 6H-SiC, Sens. Actuators B 150 (2010) 301–307.
[7] R. Pearce, T. Iakimov, M. Andersson, L. Hultman, A. Lloyd Spetz, R. Yakimova, Epitaxially grown graphene based gas sensors for ultra sensitive NO_2 detection, Sens. Actuators B 155 (2011) 451–455.
[8] G. Ko, H.Y. Kim, J. Ahn, Y.M. Park, K.Y. Lee, J. Kim, Graphene-based nitrogen dioxide gas sensors, Curr. Appl. Phys. 10 (2010) 1002–1004.
[9] M.G. Chung, D.H. Kim, H.M. Lee, T. Kim, J.H. Choi, D.K. Seo, J.B. Yoo, S.H. Hong, T.J. Kang, Y.H. Kim, Highly sensitive NO_2 gas sensor based on ozone treated graphene, Sens. Actuators B 166–167 (2012) 172–176.
[10] M. Gautam, A.H. Jayatissa, Gas sensing properties of graphene synthesized by chemical vapor deposition, Mater. Sci. Eng. C 31 (2011) 1405–1411.
[11] B.H. Chu, C.F. Lo, J. Nicolosi, C.Y. Chang, V. Chen, W. Strupinski, S.J. Pearton, F. Ren, Hydrogen detection using platinum coated graphene grown on SiC, Sens. Actuators B 157 (2011) 500–503.
[12] H.J. Yoon, D.H. Jun, J.H. Yang, Z. Zhou, S.S. Yang, M.M.C. Cheng, Carbon dioxide gas sensor using a graphene sheet, Sens. Actuators B 157 (2011) 310–313.
[13] M.C. Mcalpine, H. Ahmad, D. Wang, J.R. Heath, Highly ordered nanowire arrays on plastic substrates for ultrasensitive flexible chemical sensors, Nat. Mater. 16 (2007) 379–384.
[14] Y. Sun, H.H. Wang, High-performance, flexible hydrogen sensors that use carbon nanotubes decorated with palladium nanoparticles, Adv. Mater. 19 (2007) 2818–2823.

[15] E. Abad, S. Zampolli, S. Macro, A. Scorzoni, B. Mazzolai, A. Juarros, D. Gómez, I. Elmi, G.C. Cardinali, J.M. Gómez, F. Palacio, M. Cicioni, A. Mondini, T. Becker, I. Sayhan, Flexible tag microlab development: gas sensors integration in RFID flexible tags for food logistic, Sens. Actuators B 127 (2007) 2–7.
[16] A. Vergara, E. Llobet, J.L. Ramírez, P. Ivanov, L. Fonseca, S. Zampolli, A. Scorzoni, T. Becker, S. Marco, J. Wöllenstein, An RFID reader with onboard sensing capability for monitoring fruit quality, Sens. Actuators B 127 (2007) 143–149.
[17] C. Lee, J. Ahn, K.B. Lee, D. Kim, J. Kim, Graphene-based flexible NO_2 chemical sensors, Thin Solid Films 520 (2012) 5459–5462.
[18] M.G. Chung, D.H. Kim, D.K. Seo, T. Kim, H.U. Im, H.M. Lee, J.B. Yoo, S.H. Hong, T.J. Kang, Y.H. Kim, Flexible hydrogen sensors using graphene with palladium nanoparticle decoration, Sens. Actuators B 169 (2012) 387–392.
[19] G. Decher, J.D. Hong, J. Schmitt, Buildup of ultrathin multilayer films by a self-assembly process. III. Consecutively alternating adsorption of anionic and cationic polyelectrolytes on charged surface, Thin Solid Films 210 (1992) 831–835.
[20] G. Decher, Fuzzy nanoassemblies: toward layered polymeric multicomposites, Science 277 (1997) 1232–1237.
[21] A.A. Mamedov, N.A. Kotov, M. Prato, D.M. Guldi, J.P. Wicksted, A. Hirsch, Molecular design of strong single-wall carbon nanotube/polyelectrolyte multilayer composites, Nat. Mater. 1 (2001) 190–194.
[22] X.B. Yan, X.J. Chen, B.K. Tay, K.A. Khor, Transparent and flexible glucose biosensor via layer-by-layer assembly of multi-wall carbon nanotubes and glucose oxidase, Electrochem. Commun. 9 (2007) 1269–1275.
[23] W. Xue, T. Cui, Electrical and electromechanical characteristics of self-assembled carbon nanotube thin films on flexible substrates, Sens. Actuators A 145–146 (2008) 330–335.
[24] P.G. Su, C.T. Lee, C.Y. Chou, K.H. Cheng, Y.S. Chuang, Fabrication of flexible NO_2 sensors by layer-by-layer self-assembly of multi-walled carbon nanotubes and their gas sensing properties, Sens. Actuators B 139 (2009) 488–493.
[25] P.G. Su, C.T. Lee, C.Y. Chou, Flexible NH_3 sensors fabricated by in situ self-assembly of polypyrrole, Talanta 80 (2009) 763–769.
[26] P.G. Su, Y.S. Chuang, Flexible H_2 sensors fabricated by layer-by-layer self-assembly thin film of multi-walled carbon nanotubes and modified in situ with Pd nanoparticles, Sens. Actuators B 145 (2010) 521–526.
[27] P.G. Su, C.C. Shiu, Flexible H_2 sensor fabricated by layer-by-layer self-assembly of thin films of polypyrrole and modified in situ with Pt nanoparticles, Sens. Actuators B 157 (2011) 275–281.
[28] S.Y. Han, Y.A. Kim, Recent development of peptide coupling reagents in organic synthesis, Tetrahedron 60 (2004) 2447–2467.
[29] N.B. Li, J.H. Park, K. Park, S.J. Kwon, H. Shin, J. Kwak, Characterization and electrocatalytic properties of Prussian blue electrochemically deposited on nano-Au/PAMAM dendrimer-modified gold electrode, Biosens. Bioelectron. 23 (2008) 1519–1526.
[30] P.G. Su, H.C. Hsu, C.Y. Liu, Layer-by-layer anchoring of copolymer of methyl methacrylate and [3-(methacrylamino)propyl] trimethyl ammonium chloride to gold surface on flexible substrate for sensing humidity, Sens. Actuators B 178 (2013) 289–295.
[31] J. Ito, J. Nakamura, A. Natori, Semiconducting nature of the oxygen-adsorbed graphene sheet, J. Appl. Phys. 103 (2008) 113712–113715.
[32] F. Schedin, A.K. Geim, S.V. Morozov, E.W. Hill, P. Blake, M.I. Katsnelson, K.S. Novoselov, Detection of individual gas molecules adsorbed on grapheme, Nat. Mater. 6 (2007) 652–655.
[33] O. Leenaerts, B. Partoens, F.M. Peeters, Adsorption of H_2O, NH_3, CO NO_2 and NO on graphene: a first-principles study, Phys. Rev. B 77 (2008) 125416–125426.
[34] E.W. Hill, A. Vijayaragahvan, K. Novoselov, Graphene sensors, IEEE Sensor J. 11 (2011) 3161–3170.
[35] J. Moser, A. Verdaguer, D. Jiménez, A. Barreiro, A. Bachtold, The environment of graphene by electrostatic force microscopy, Appl. Phys. Lett. 92 (2008) 123507–123513.
[36] T.O. Wehling, M.I. Katsnelson, A.I. Lichtenstein, Adsorbates on graphene: impurity states and electron scattering, Chem. Phys. Lett. 476 (2009) 125–134.
[37] Y. Dan, Y. Lu, N.J. Kybert, Z. Luo, A.T.C. Johnson, Intrinsic response of graphene vapor sensors, Nano Lett. 9 (2009) 1472–1475.
[38] G. Casalbore-Miceli, M.J. Yang, N. Camaioni, C.M. Mari, Y. Li, H. Sun, M. Ling, Investigations on the ion transport mechanism in conduction polymer films, Solid State Ionics 131 (2000) 311–321.
[39] P.G. Su, S.C. Huang, Electrical and humidity sensing properties of carbon nanotubes-SiO_2-poly(2-acrylamido-2-methylpropane sulfonate) composite material, Sens. Actuators B 113 (2006) 142–149.

Biographies

Pi-Guey Su is currently a professor in Department of Chemistry at Chinese Culture University. He received his BS degree from Soochow University in Chemistry in 1993 and PhD. degree in Chemistry from National Tsing Hua University in 1998. He worked as a researcher in Industrial Technology Research Institute, Taiwan, from 1998 to 2002. He joined as an assistant professor in the General Education Center, Chungchou Institute of Technology from 2003 to 2005. He worked as an assistant professor in Department of Chemistry at Chinese Culture University from 2005 to 2007. He worked as an associate professor in Department of Chemistry at Chinese Culture University from 2007 to 2010. His fields of interests are chemical sensors, gas and humidity sensing materials and humidity standard technology.

Hung-Chiang Shieh received a BS degree in Chemistry from Chinese Culture University in 2010. He entered the MS course of Chemistry at Chinese Culture University in 2010. His main areas of interest are gas sensing materials.